Open string Regge trajectory and its field theory limit

Francisco Rojas and Charles B. Thorn

Phys. Rev. D **84**, 026006 — Published 21 July 2011

DOI: 10.1103/PhysRevD.84.026006

The Open String Regge Trajectory and Its Field Theory Limit[1]

Francisco Rojas[2] and Charles B. Thorn[3]

Institute for Fundamental Theory
Department of Physics, University of Florida, Gainesville FL 32611

Abstract

We study the properties of the leading Regge trajectory in open string theory including the open string planar one-loop corrections. With $SU(N)$ Chan-Paton factors, the sum over planar open string multi-loop diagrams describes the 't Hooft limit $N \to \infty$ with Ng_s^2 fixed. Our motivation is to improve the understanding of open string theory at finite α' as a model of gauge field theories. $SU(N)$ gauge theories in D space-time dimensions are described by requiring open strings to end on a stack of N Dp-branes of space-time dimension $D = p+1$. The large N leading trajectory $\alpha(t) = 1 + \alpha' t + \Sigma(t)$ can be extracted, through order g^2, from the $s \to -\infty$ limit, at fixed t, of the four open string tree and planar loop diagrams. We analyze the $t \to 0$ behavior with the result that $\Sigma(t) \sim -Cg^2(-\alpha' t)^{(D-4)/2}/(D-4)$. This result precisely tracks the 1-loop Reggeized gluon of gauge theory in $D > 4$ space-time dimensions. In particular, for $D \to 4$ it reproduces the known infrared divergences of gauge theory in 4 dimensions with a Regge trajectory behaving as $-\ln(-\alpha' t)$. We also study $\Sigma(t)$ in the limit $t \to -\infty$ and show that, when $D < 8$, it behaves as $\alpha' t/(\ln(-\alpha' t))^\gamma$, where $\gamma > 0$ depends on D and the number of massless scalars. Thus, as long as $4 < D < 8$, the 1-loop correction stays small relative to the tree trajectory for $-\alpha' t$ arbitrarily large. Finally we present the results of numerical calculations of $\Sigma(t)$ for all negative t.

---

[1] Supported in part by the Department of Energy under Grant No. DE-FG02-97ER-41029.
[2] E-mail address: `frojasf@phys.ufl.edu`
[3] E-mail address: `thorn@phys.ufl.edu`

1 Introduction

Ever since the early days of dual resonance models, it has been recognized that quantum field theory can be recovered from those models as the zero slope (infinite string tension) limit [1, 2]. In more recent years this field/string relationship has been exploited to motivate the AdS/CFT correspondence [3], in which the closed strings remain stringy even in the zero-slope limit: in this limit, closed superstring theory on an $\mathrm{AdS}_5 \times \mathrm{S}_5$ background with a coincident stack of D3-branes is then conjectured to be equivalent to $\mathcal{N} = 4$ supersymmetric Yang-Mills theory. This conjecture is buttressed by the ability to do explicit calculations at weak coupling via the gauge theory loop expansion and at strong coupling via a semiclassical treatment of the closed string on AdS.

However, gauge theories with less or no supersymmetry ($0 \leq \mathcal{N} < 4$) are also zero slope limits of corresponding open string theories. We think it is reasonable to expect the techniques of string theory to deepen our dynamical understanding of these theories too. Without maximal supersymmetry, quantum effects typically break the conformal symmetry of the classical gauge theory, linking the effective coupling to the scale of the process studied. The coupling constant ceases to be an adjustable parameter: at high momenta the coupling is weak and field theoretic perturbation theory is applicable. However, at low momenta the coupling is at least of order 1, though not necessarily very large. Unlike the conformal theories, this means that semi-classical string methods, controlled by the infinite coupling limit, cannot be reliably applied to the putative closed string theory which might represent such a gauge theory.

Under these circumstances, we think a useful line of attack is to replace the field theory with its corresponding open string theory, delaying the $\alpha' \to 0$ limit to the end of the calculation. In other words, we seek to resolve nonperturbative issues in gauge theory by summing open string multiloop diagrams instead of field theoretic multi-loop diagrams. Since closed string intermediate states inevitably participate in nonplanar open string diagrams, we expect this approach to be most fruitful for the summation of planar open string diagrams only. That is, we expect this approach to teach us the most about gauge theories in 't Hooft's large N limit [4].

Keeping $\alpha' > 0$ can be viewed as a regularization procedure for the program developed in [5, 6] to represent and sum the planar diagrams of gauge theory on a lightcone worldsheet lattice [7]. In this representation the gluon is replaced by a kind of topological open string whose only physical energy eigenstate is the spin one massless gluon. In practice, however, the lightcone lattice produces ultraviolet artifacts, the cancellation of which requires worldsheet counterterms beyond coupling and wave function renormalization [8, 9]. It seems likely that more and more such counterterms will be needed at each order of perturbation theory. Since the excitations of the topological string cancel in the worldsheet path integral, they have no mitigating effect on the field theoretic ultraviolet divergences. In contrast, with $\alpha' > 0$ the open string excitations are real, and they do soften the ultraviolet divergences.

With this application in mind, it behooves us to understand perturbative open string theory as well as we understand perturbative gauge theory. In this article we begin this task with a study of one loop open string physics. As a concrete example we focus on the one loop correction to the leading open string Regge trajectory[4]. Writing $\alpha(t) = \alpha' t + 1 + \Sigma(t)$ with $\Sigma(t) = O(g^2)$, we see that the zero slope limit of Σ should just describe the known reggeization of the gauge particle (which we call the gluon in this article). With our new viewpoint, we prefer to think of $\alpha(t)$ as a fundamental physical quantity in open string theory with $\alpha' > 0$ and fixed. Then the reggeized gauge theory gluon is simply the part of this trajectory near $t = 0$. But the trajectory away from $t = 0$ is also significant to open string physics. Therefore we study both the small and large t behavior of Σ analytically. And we also carry out numerical calculations for the whole range of negative t.

We organize the paper as follows. In section 2 we recall the one loop amplitude for the Neveu-Schwarz model [11, 12], as calculated long ago [13]. In order to obtain the gauge theories in D space-time dimensions as zero slope limits, we adapt that calculation in several ways. First of all we work in the critical dimension throughout: the interior points of the open string are allowed to move in 10 spacetime dimensions. This greatly simplifies the elimination of unphysical states from the loop [14, 15]. Open string tachyons are

[4]This choice is inspired by recent work on the gluon Regge trajectory in the context of the AdS/CFT correspondence [10].

eliminated by working in the even G-parity subspace of open string states [16] and projecting out odd G-parity states in the loop. To get a D-dimsnsional zero slope limit, we require each open string to end on Dp-branes, with $p = D - 1$ and D the spacetime dimension of the branes[5]. Finally, when $D < 10$ we arrange for only $S \leq 10 - D$ massless scalars to circulate in the loop.[6] This extends the applicability of our methods to pure gauge theory, $S = 0$. These various projections are summarized by writing out the partition functions in the $\mathcal{F}_2$ open string state space [12]

$$Z \quad = \quad \mathrm{Tr} w^{L_0 - 1/2} = \frac{w^{-1/2}}{2}\left[\frac{(1-w^{1/2})^{10-D-S}}{\ln^{D/2} w}\frac{\prod(1+w^r)^8}{\prod(1-w^n)^8} - \frac{(1+w^{1/2})^{10-D-S}}{\ln^{D/2} w}\frac{\prod(1-w^r)^8}{\prod(1-w^n)^8}\right] \tag{1}$$

where the products are over $n = 1, 2, \cdots$ and $r = 1/2, 3/2, \cdots$. Working with these results, and following the methods of [18–20], we extract the one-loop correction Σ to the open string Regge trajectory in Section 3.

We then turn to a detailed study of the properties of Σ. Section 4 is devoted to a study of the small t behavior of Σ. This limit exposes the infrared structure of the open string theory, which is identical to that of the corresponding gauge theory. As long as $D > 4$ infrared divergences are absent, and we confirm that $\Sigma(0) = 0$, a reflection of the zero mass of the gluon. In Section 5 we study the large t behavior of $\Sigma(t)$, which exposes the ultraviolet structure of open string theory. Although this is not the same as the ultraviolet structure of the gauge theory, it shares a common property as long as $D < 8$: ultraviolet divergences can be absorbed in coupling renormalization. For $D \geq 8$ subleading divergences require renormalization of the Regge slope parameter α'. In Section 6 we describe our numerical work, illustrating it with graphs of $\Sigma(t)$ in various regimes. We close with discussion and concluding remarks in Section 7.

2 The One Loop Correction

The open string coupling g will be normalized in this paper so that in the zero-slope limit it is related to the QCD strong coupling g_s by $\alpha_s N = g_s^2 N/4\pi = g^2/2\pi$. Thus g will be fixed in the large N limit. Then the properly normalized M gluon open string one loop planar amplitude for the even G-parity Neveu-Schwarz (NS+) model [13, 21] is $(g\sqrt{2\alpha'})^M$ times

$$\mathcal{M}_M = \frac{1}{2}(\mathcal{M}_M^+ - \mathcal{M}_M^-) \tag{2}$$

where

$$\begin{aligned}\mathcal{M}_M^\pm \quad = \quad & \int \frac{dw}{w}\prod_{i=2}^M \frac{dy_i}{y_i} w^{-1/2}\left(\frac{-1}{4\pi\alpha' \ln w}\right)^{D/2} \exp\left\{\alpha' \sum_{i<j} k_i \cdot k_j \frac{\ln^2 y_i/y_j}{\ln w}\right\} \\ & (1 \mp w^{1/2})^{10-D-S} \langle \hat{\mathcal{P}}(y_1)\cdots\hat{\mathcal{P}}(y_M)\rangle^\pm \frac{\prod_r (1 \pm w^r)^8}{\prod_n (1-w^n)^8}\prod_{i<j}\left[2i\frac{\theta_1\left(-i\ln\sqrt{y_i/y_j}, \sqrt{w}\right)}{\theta_1'(0,\sqrt{w})}\right]^{2\alpha' k_i\cdot k_j}\end{aligned} \tag{3}$$

[5] Another way would be to compactify $10 - D$ dimensions. Such an approach would yield a Regge trajectory correction $\Sigma(t)$ with the same small t behavior but different large t behavior compared to our model. The D-brane approach is superior because it introduces the fewest arbitrary features in the parent string theory (Occam's razor).

[6] For simplicity, in the following we shall use the nonabelian D-brane projection proposed in [17]. Another approach is to retain only states even under $b_r^A, a_n^A \to -b_r^A, -a_n^A$ where $D + S < A \leq 10$. In this case, the following changes occur in Z:

$$(1-w^{1/2})^{10-D-S}\frac{\prod(1+w^r)^8}{\prod(1-w^n)^8} \to \frac{1}{2}\left[\frac{\prod(1+w^r)^8}{\prod(1-w^n)^8} + \frac{\prod(1+w^r)^{D-2+S}\prod(1-w^r)^{10-D-S}}{\prod(1-w^n)^{D-2+S}\prod(1+w^n)^{10-D-S}}\right]$$

$$(1+w^{1/2})^{10-D-S}\frac{\prod(1-w^r)^8}{\prod(1-w^n)^8} \to \frac{1}{2}\left[\frac{\prod(1-w^r)^8}{\prod(1-w^n)^8} + \frac{\prod(1-w^r)^{D-2+S}\prod(1+w^r)^{10-D-S}}{\prod(1-w^n)^{D-2+S}\prod(1+w^n)^{10-D-S}}\right]$$

where we use the notation and conventions of [22]. The integration range for the Koba-Nielsen variables y_i is given by

$$0 < w < y_M < y_{M-1} < \cdots < y_2 < y_1 = 1 \,. \tag{4}$$

We have adapted the standard planar open string one loop calculation in 10 space-time dimensions to open strings ending on a stack of N coincident Dp-branes for $p = D - 1$. In the planar one-loop calculation, this simply amounts to integrating over only the first D components of the loop momentum and setting the remaining components to zero. We also arrange that there are $S \leq 10 - D$ massless scalars, achieved here by the extra factors of $(1 \mp w^{1/2})$ as dictated by the non-abelian D-brane projection described in [17]. The factors involving the Jacobi θ_1 function have the infinite product representation

$$\prod_{i<j} y_j^{2\alpha' k_i\cdot k_j} \prod_{i<j}\left[2i\frac{\theta_1\left(-i\ln\sqrt{y_i/y_j},\sqrt{w}\right)}{\theta_1'(0,\sqrt{w})}\right]^{2\alpha' k_i\cdot k_j} = \prod_{i<j}\left[\left(1-\frac{y_j}{y_i}\right)\prod_n \frac{(1-w^n y_i/y_j)\,(1-w^n y_j/y_i)}{(1-w^n)^2}\right]^{2\alpha' k_i\cdot k_j} . \tag{5}$$

The gluon vertex operator is $V = e^{ik\cdot x}(\epsilon\cdot\mathcal{P} + \sqrt{2\alpha'}k\cdot H\epsilon\cdot H) \equiv e^{ik\cdot x}\hat{\mathcal{P}}$. The $\langle\cdots\rangle$ is a correlator of a finite number of $\mathcal{P}$ and H worldsheet fields determined by its Wick expansion with the following contraction rules

$$\begin{aligned}
\langle\mathcal{P}(y_l)\rangle &= \sqrt{2\alpha'}\sum_i k_i\left[-\frac{\ln(y_i/y_l)}{\ln w} + \frac{1}{2}\frac{y_i+y_l}{y_l-y_i} + \sum_{n=1}^{\infty}\left(\frac{y_i w^n}{y_l - y_i w^n} - \frac{y_l w^n}{y_i - y_l w^n}\right)\right]\\
\langle\mathcal{P}^\mu(y_i)\mathcal{P}^\nu(y_l)\rangle &= \langle\mathcal{P}^\mu(y_i)\rangle\langle\mathcal{P}^\nu(y_l)\rangle + \eta^{\mu\nu}\left[-\frac{1}{\ln w} + \frac{y_i y_l}{(y_i-y_l)^2} + \sum_{n=1}^{\infty}\left(\frac{y_i y_l w^n}{(y_l - y_i w^n)^2} + \frac{y_i y_l w^n}{(y_i - y_l w^n)^2}\right)\right]\\
\langle H^\mu(y_i)H^\nu(y_j)\rangle^+ &= \eta^{\mu\nu}\sum_r \frac{(y_j/y_i)^r + (w y_i/y_j)^r}{1+w^r}\\
\langle H^\mu(y_i)H^\nu(y_j)\rangle^- &= \eta^{\mu\nu}\sum_r \frac{(y_j/y_i)^r - (w y_i/y_j)^r}{1-w^r}.
\end{aligned} \tag{6}$$

The $\pm$ superscript on the H contractions distinguishes the two types of traces over the b_r oscillators: for $+$ odd and even G-parity states contribute with the same sign, whereas for $-$ they contribute with opposite signs. In the $\mathcal{F}_2$ picture, the difference of the two traces projects out the odd G-parity states.

Finally we present the one-loop amplitude in the natural cylinder variables, $\theta_i = \pi\ln y_i/\ln w$ and $\ln q = 2\pi^2/\ln w$,

$$\mathcal{M}_M^+ = 2^M\left(\frac{1}{8\pi^2\alpha'}\right)^{D/2}\int\prod_{k=2}^M d\theta_k\int_0^1\frac{dq}{q} \left(\frac{-\pi}{\ln q}\right)^{(10-D)/2} P_+(q)\prod_{l<m}\left[\psi(\theta_m-\theta_l,q)\right]^{2\alpha' k_l\cdot k_m}\langle\hat{\mathcal{P}}_1\hat{\mathcal{P}}_2\cdots\hat{\mathcal{P}}_M\rangle^+ \tag{7}$$

$$\mathcal{M}_M^- = 2^M\left(\frac{1}{8\pi^2\alpha'}\right)^{D/2}\int\prod_{k=2}^M d\theta_k\int_0^1\frac{dq}{q} \left(\frac{-\pi}{\ln q}\right)^{(10-D)/2} P_-(q)\prod_{l<m}\left[\psi(\theta_m-\theta_l,q)\right]^{2\alpha' k_l\cdot k_m}\langle\hat{\mathcal{P}}_1\hat{\mathcal{P}}_2\cdots\hat{\mathcal{P}}_M\rangle^- \tag{8}$$

where we have defined

$$
\begin{aligned}
P_+(q) &\equiv q^{-1}(1-w^{1/2})^{10-D-S}\frac{\prod_r(1+q^{2r})^8}{\prod_n(1-q^{2n})^8}, \qquad P_-(q)\equiv 2^4(1+w^{1/2})^{10-D-S}\frac{\prod_n(1+q^{2n})^8}{\prod_n(1-q^{2n})^8} && (9)\\
\psi(\theta,q) &= \sin\theta\prod_n\frac{(1-q^{2n}e^{2i\theta})(1-q^{2n}e^{-2i\theta})}{(1-q^{2n})^2}, \qquad \hat{\mathcal{P}}=\epsilon\cdot\mathcal{P}+\sqrt{2\alpha'}k\cdot H\epsilon\cdot H, && (10)
\end{aligned}
$$

and where the average $\langle\cdots\rangle$ is evaluated with contractions:

$$
\begin{aligned}
\langle\mathcal{P}_l\rangle &= \sqrt{2\alpha'}\sum_i k_i\left[\frac{1}{2}\cot\theta_{il}+\sum_{n=1}^{\infty}\frac{2q^{2n}}{1-q^{2n}}\sin 2n\theta_{il}\right] && (11)\\
\langle\mathcal{P}_i\mathcal{P}_l\rangle-\langle\mathcal{P}_i\rangle\langle\mathcal{P}_l\rangle &= \frac{1}{4}\csc^2\theta_{il}-\sum_{n=1}^{\infty}n\frac{2q^{2n}}{1-q^{2n}}\cos 2n\theta_{il} && (12)\\
\langle H_iH_j\rangle^+ &\equiv \chi_+(\theta_{ji})=\frac{1}{2\sin\theta_{ji}}-2\sum_r\frac{q^{2r}\sin 2r\theta_{ji}}{1+q^{2r}}=\frac{1}{2}\theta_2(0)\theta_4(0)\frac{\theta_3(\theta_{ji})}{\theta_1(\theta_{ji})} && (13)\\
\langle H_iH_j\rangle^- &\equiv \chi_-(\theta_{ji})=\frac{\cos\theta_{ji}}{2\sin\theta_{ji}}-2\sum_n\frac{q^{2n}\sin 2n\theta_{ji}}{1+q^{2n}}=\frac{1}{2}\theta_3(0)\theta_4(0)\frac{\theta_2(\theta_{ji})}{\theta_1(\theta_{ji})}\,. && (14)
\end{aligned}
$$

We have abbreviated $\theta_{ji}=\theta_j-\theta_i$ and we have again suppressed space-time indices. Finally the range of integration is

$$
0=\theta_1<\theta_2<\cdots<\theta_N<\pi. \tag{15}
$$

In these formulas r ranges over positive half odd integers, n over positive integers, and $l,m\in[1,\cdots,M]$.

The worst divergence in the q integration near $q=0$, the q^{-2} behavior in $\mathcal{M}^+$, can be cancelled by the Neveu-Scherk counterterm [23]

$$
\begin{aligned}
\mathcal{C}_M &= 2^M\left(\frac{1}{8\pi^2\alpha'}\right)^{D/2}\int\prod_{k=2}^{M}d\theta_k\int_0^1\frac{dq}{q}\\
&\qquad\left(\frac{-\pi}{\ln q}\right)^{(10-D)/2}P_+(q)\prod_{l<m}\left[\sin\theta_m-\theta_l\right]^{2\alpha' k_l\cdot k_m}\langle\hat{\mathcal{P}}_1\hat{\mathcal{P}}_2\cdots\hat{\mathcal{P}}_M\rangle_C && (16)
\end{aligned}
$$

where the average is evaluated with the contractions

$$
\begin{aligned}
\langle\mathcal{P}_l\rangle_C &= \sqrt{2\alpha'}\sum_i k_i\left[\frac{1}{2}\cot\theta_{il}\right], \qquad \langle\mathcal{P}_i\mathcal{P}_l\rangle_C-\langle\mathcal{P}_i\rangle_C\langle\mathcal{P}_l\rangle_C=\frac{1}{4}\csc^2\theta_{il}\\
\langle H_iH_j\rangle_C &= \frac{1}{2\sin\theta_{ji}}
\end{aligned}
$$

The θ_i integrals, which are formally divergent because of on-shell kinematics, require a regularization procedure to be well-defined. In this paper we employ the GNS prescription, which is to temporarily suspend momentum conservation $\sum_i k_i=P$ and analytically continue to $P=0$ after integration [23, 24]. As shown long ago [23], this regularization keeps the gluon massless through 1 loop, a necessary requirement of gauge invariance. While its effectiveness at preserving gauge invariance has not been proven beyond one loop, we believe it should work in the context of the open string planar multi-loop diagrams needed to describe the $N\to\infty$ limit. With GNS regularization at one loop, the Neveu-Scherk counterterm simply goes to the tree amplitude [23]. This establishes that this leading divergence can be absorbed in renormalization of the coupling constant. If the brane space-time dimension $D<8$, there are no subleading ultraviolet divergences. Furthermore if $D>4$ there are no infrared divergences: after coupling renormalization the loop integral is completely finite for $D=5,6,7$, and has only infrared divergences for $D\le 4$.

As we have explained the θ integrals are well-defined through analytic continuation from $P \neq 0$. However, it is useful in the following to be able to deal with well-defined expressions at $P = 0$. This can be accomplished in an unambiguous way by taking $P \neq 0$ and then subtracting and adding the Neveu-Scherk counterterm: $I(P) = (I(P) - C(P)) + C(P)$. Then it is safe to take $P \to 0$ in the first two terms. The $P \to 0$ limit of the last term $C(P)$ can be carefully studied, to trace the effects of the divergence.

3 The Open String Regge Trajectory

In general, the correction to the tree level Regge trajectory can be read off from the large s at fixed t behavior of the one loop amplitude [18–20]. Assuming Regge behavior of the exact amplitude 4 particle amplitude,

$$(\beta(t) + \delta\beta)s^{\alpha(t)+\delta\alpha} \approx \beta s^{\alpha} + \delta\alpha\beta s^{\alpha}\ln s + \delta\beta s^{\alpha}, \tag{17}$$

$\delta\alpha$ is just the coefficient of $\beta s^{\alpha}\ln s$ in the one loop amplitude.

3.1 Regge Asymptotics for the 1 Loop Amplitudes

The large s behavior of $\mathcal{M}_4^{\pm}$ is controlled by the region $\theta_{23}, \theta_{41} \approx 0$ or $\theta_2 \approx \theta_3$ and $\theta_4 \approx \pi$. The polarization factors of the Regge contribution to the tree amplitude are $\epsilon_2 \cdot \epsilon_3 \epsilon_1 \cdot \epsilon_4$, so we pick out those terms in the correlator. We find, after a little algebra,

$$\begin{aligned} \langle \hat{\mathcal{P}}_1\hat{\mathcal{P}}_2\hat{\mathcal{P}}_3\hat{\mathcal{P}}_4\rangle \quad \to \quad & \epsilon_2 \cdot \epsilon_3 \epsilon_1 \cdot \epsilon_4 \Big((\langle \mathcal{P}_2\mathcal{P}_3\rangle + \alpha' t\langle H_2H_3\rangle^2)(\langle \mathcal{P}_1\mathcal{P}_4\rangle + \alpha' t\langle H_1H_4\rangle^2) \\ & + \langle H_2H_3\rangle\langle H_1H_4\rangle \left[\alpha'^2 s^2\langle H_1H_2\rangle\langle H_3H_4\rangle - \alpha'^2(s+t)^2\langle H_1H_3\rangle\langle H_2H_4\rangle\right] \Big) \end{aligned} \tag{18}$$

We next list the asymptotic behaviors of the various factors in the correlator in the limit $\theta_{32} \to 0, \theta_{41} \to \pi$:

$$\begin{aligned} \langle \mathcal{P}_1\mathcal{P}_4\rangle \quad &\sim \quad \frac{1}{4(\pi - \theta_4)^2}, \qquad \langle \mathcal{P}_2\mathcal{P}_3\rangle \sim \frac{1}{4(\theta_3 - \theta_2)^2} \\ \langle H_1H_4\rangle^{\pm} \quad &\sim \quad \frac{\pm 1}{2(\pi - \theta_4)}, \qquad \langle H_2H_3\rangle^{\pm} \sim \frac{1}{2(\theta_3 - \theta_2)}, \qquad \langle H_1H_3\rangle^{\pm} = \chi_{\pm}(\theta_3) \\ \langle H_1H_2\rangle^{\pm} \quad &= \quad \chi_{\pm}(\theta_3 - \theta_{32}) \sim \chi_{\pm}(\theta_3) - \theta_{32}\chi'_{\pm}(\theta_3) + \frac{\theta_{32}^2}{2}\chi''_{\pm}(\theta_3) \\ \langle H_3H_4\rangle^{\pm} \quad &= \quad \pm\chi_{\pm}(\theta_3 + (\pi - \theta_4)) \sim \pm\left(\chi_{\pm}(\theta_3) + (\pi - \theta_4)\chi'_{\pm}(\theta_3) + \frac{(\pi - \theta_4)^2}{2}\chi''_{\pm}(\theta_3)\right) \\ \langle H_2H_4\rangle^{\pm} \quad &= \quad \pm\chi_{\pm}(\theta_3 + (\pi - \theta_4) - \theta_{32}) \sim \pm\left(\chi_{\pm}(\theta_3) + (\pi - \theta_4 - \theta_{32})\chi'_{\pm}(\theta_3) + \frac{(\pi - \theta_4 - \theta_{32})^2}{2}\chi''_{\pm}(\theta_3)\right) \end{aligned}$$

Notice that the coefficient of s^2 inside the square brackets on the second line of (18) simplifies dramatically

$$\langle H_1H_2\rangle\langle H_3H_4\rangle - \langle H_1H_3\rangle\langle H_2H_4\rangle \quad \sim \quad \pm\theta_{32}(\pi - \theta_4)(\chi_{\pm}(\theta_3)\chi''_{\pm}(\theta_3) - \chi'^2_{\pm}(\theta_3)) \tag{19}$$

Putting these forms into the correlator we have the asymptotics

$$\begin{aligned} \langle \hat{\mathcal{P}}_1\hat{\mathcal{P}}_2\hat{\mathcal{P}}_3\hat{\mathcal{P}}_4\rangle \quad \sim \quad & \epsilon_2 \cdot \epsilon_3 \epsilon_1 \cdot \epsilon_4 \Bigg(\frac{(1 + \alpha' t)^2}{16\theta_{32}^2(\pi - \theta_4)^2} + \frac{1}{4}(\alpha' s)^2(\chi_{\pm}(\theta_3)\chi''_{\pm}(\theta_3) - \chi'^2_{\pm}(\theta_3)) \\ & - \alpha'^2\chi^2_{\pm}(\theta_3)\frac{2st + t^2}{4\theta_{32}(\pi - \theta_4)} \Bigg) \end{aligned} \tag{20}$$

The s dependent factors in the four string 1-loop diagram involve the combination:

$$\begin{aligned}\frac{\psi(\theta_{43})\psi(\theta_{21})}{\psi(\theta_{42})\psi(\theta_{31})} &= \frac{\psi(\theta_3+(\pi-\theta_4))\psi(\theta_3-\theta_{32})}{\psi(\theta_3-\theta_{32}+(\pi-\theta_4))\psi(\theta_{31})} \sim \exp\left\{-\theta_{32}(\pi-\theta_4)\left(\frac{\psi'^2}{\psi^2}-\frac{\psi''}{\psi}\right)\right\} \\ \left(\frac{\psi(\theta_{43})\psi(\theta_{21})}{\psi(\theta_{42})\psi(\theta_{31})}\right)^{-\alpha' s} &\sim \exp\{-\alpha' s\;\theta_{32}(\pi-\theta_4)(\ln\psi)''\}\end{aligned} \tag{21}$$

Meanwhile the t dependence is given by the factor

$$\left(\frac{\psi(\theta_{41})\psi(\theta_{32})}{\psi(\theta_{42})\psi(\theta_{31})}\right)^{-\alpha' t} \sim \left(\frac{\theta_{32}(\pi-\theta_4)}{\psi^2(\theta_3)}\right)^{-\alpha' t} \tag{22}$$

Taking $s\to-\infty$, the $\theta_{32},\theta_4\equiv\pi-\hat\theta_4$ integrals are dominated by small $\theta_{23}\approx 0$, $\hat\theta_4\approx 0$, and hence can be done by using

$$\begin{aligned}\int_0^\epsilon d\xi\int_0^\epsilon d\eta(\xi\eta)^a e^{-\xi\eta\kappa} &= \int_0^\epsilon\frac{d\xi}{\xi}\int_0^{\xi\epsilon}d\eta\eta^a e^{-\eta\kappa} = \kappa^{-a-1}\int_0^{\epsilon^2\kappa}d\eta\eta^a\ln\frac{\epsilon^2\kappa}{\eta}e^{-\eta\kappa} \\ &\sim \Gamma(a+1)\kappa^{-a-1}\ln\kappa, \qquad \kappa\to\infty\end{aligned} \tag{23}$$

We use this formula for $\kappa=(-\alpha' s)(-[\ln\psi]'')$ and $a=-\alpha' t-2,-\alpha' t-1,-\alpha' t$:

$$\begin{aligned}\mathcal{M}_4^+ &\sim 4\epsilon_2\cdot\epsilon_3\epsilon_1\cdot\epsilon_4\left(\frac{1}{8\pi^2\alpha'}\right)^{D/2}\int_0^1\frac{dq}{q}\left(\frac{-\pi}{\ln q}\right)^{(10-D)/2}P_+(q) \\ &\quad \Gamma(-\alpha' t)(-\alpha' s)^{1+\alpha' t}\ln(-\alpha' s)\int d\theta_3(-\psi^2(\theta_3)[\ln\psi]'')^{\alpha' t} \\ &\quad \left(-\frac{1}{4}(1+\alpha' t)[-\ln\psi]''-\alpha' t\frac{\chi_+(\theta_3)\chi_+''(\theta_3)-\chi_+'^2(\theta_3)}{[-\ln\psi]''}+2\alpha' t\chi_+^2(\theta_3)\right) \\ \mathcal{M}_4^- &\sim 4\epsilon_2\cdot\epsilon_3\epsilon_1\cdot\epsilon_4\left(\frac{1}{8\pi^2\alpha'}\right)^{D/2}\int_0^1\frac{dq}{q}\left(\frac{-\pi}{\ln q}\right)^{(10-D)/2}P_-(q) \\ &\quad \Gamma(-\alpha' t)(-\alpha' s)^{1+\alpha' t}\ln(-\alpha' s)\int d\theta_3(-\psi^2(\theta_3)[\ln\psi]'')^{\alpha' t} \\ &\quad \left(-\frac{1}{4}(1+\alpha' t)[-\ln\psi]''-\alpha' t\frac{\chi_-(\theta_3)\chi_-''(\theta_3)-\chi_-'^2(\theta_3)}{[-\ln\psi]''}+2\alpha' t\chi_-^2(\theta_3)\right)\end{aligned} \tag{24}$$

We recall that the total planar 1-loop amplitude is given by

$$\mathcal{M}_4^{1\text{ loop}} = (g\sqrt{2\alpha'})^4\frac{\mathcal{M}_4^+-\mathcal{M}_4^-}{2}. \tag{25}$$

3.2 Extraction of the Regge Trajectory

In order to extract the correction to the Regge trajectory we need to combine the Regge behavior of the one loop diagram and that of the tree:

$$\mathcal{M}_4^{\text{Tree}}+\mathcal{M}_4^{1\text{ loop}} \sim -2g^2\epsilon_2\cdot\epsilon_3\epsilon_1\cdot\epsilon_4\Gamma(-\alpha' t)(-\alpha' s)^{1+\alpha' t}\left(1+\Sigma(t)\ln(-\alpha' s)\right), \tag{26}$$

where $\Sigma=(\Sigma^+-\Sigma^-)/2$ with

$$\begin{aligned}\Sigma^+ &= -\frac{8g^2\alpha'^{2-D/2}}{(8\pi^2)^{D/2}}\int_0^1\frac{dq}{q}\left(\frac{-\pi}{\ln q}\right)^{(10-D)/2}P_+(q) \\ &\quad \int_0^\pi d\theta\left((-\psi^2(\theta)[\ln\psi]'')^{\alpha' t}\frac{\alpha' t}{[\ln\psi]''}X^+-\frac{1}{4}(-\psi^2(\theta)[\ln\psi]'')^{\alpha' t}[-\ln\psi]''+\frac{1}{4\sin^2\theta}\right)\end{aligned} \tag{27}$$

$$
\begin{aligned}
\Sigma^- &= -\frac{8g^2\alpha'^{2-D/2}}{(8\pi^2)^{D/2}}\int_0^1 \frac{dq}{q}\left(\frac{-\pi}{\ln q}\right)^{(10-D)/2} P_-(q) \\
&\int_0^\pi d\theta\bigg((-\psi^2(\theta)[\ln\psi]'')^{\alpha' t}\frac{\alpha' t}{[\ln\psi]''}X^- - \frac{1}{4}(-\psi^2(\theta)[\ln\psi]'')^{\alpha' t}[-\ln\psi]'' + \frac{1}{4\sin^2\theta}\bigg)\,. \qquad (28)
\end{aligned}
$$

where we have defined

$$
X^\pm \equiv \frac{1}{4}[-\ln\psi]''^2 + \chi_\pm(\theta)\chi''_\pm(\theta) - \chi'^2_\pm(\theta) - 2\chi^2_\pm(\theta)[-\ln\psi]'' \qquad (29)
$$

It is remarkable that, contrary to appearances, $X^\pm$ are independent of θ (see the Appendix).

We have included the Neveu-Scherk subtraction terms in the integrands of both $\Sigma^\pm$ in order that the θ integrals are explicitly finite: they are obtained via the substitutions

$$
\begin{aligned}
\psi \to \psi_C = \sin\theta, \qquad \chi^+ &\to \chi_C = \frac{1}{2\sin\theta} \\
-\psi_C^2[\ln\psi_C]'' &= 1 \\
\frac{1}{4}(1+\alpha' t)[-\ln\psi_C]'' + \alpha' t\frac{\chi_C\chi''_C - \chi''_C}{[-\ln\psi_C]''} - 2\alpha' t\chi^2_C &= \frac{1}{4\sin^2\theta} \qquad (30)
\end{aligned}
$$

In fact these subtraction terms are actually zero with the GNS regulator. That is, doing the integral with $P \neq 0$ and then continuing to $P = 0$ gives

$$
\int_0^{2\pi} d\theta(\sin\theta/2)^{P^2-2} = \frac{\Gamma(1/2)\Gamma((P^2-1)/2)}{\Gamma(P^2/2)} \to 0, \qquad \text{for } P \to 0. \qquad (31)
$$

It is important to keep the subtraction terms in the integrands because we want to use the integral representations for $\Sigma^\pm$ at $P = 0$.

Furthermore as pointed out by Neveu and Scherk [23], when $t = 0$ the θ integral of the last terms in the expressions for $\Sigma^\pm$ gives zero:

$$
\int_0^\pi d\theta\left([\ln\psi]'' + \frac{1}{\sin^2\theta}\right) = \left([\ln\psi]' - \cot\theta\right)\big|_0^\pi = \left(\sum_{n=1}^\infty \frac{4q^{2n}\sin 2\theta}{1-2q^{2n}\cos 2\theta + q^{4n}}\right)\bigg|_0^\pi = 0 \qquad (32)
$$

Thus we can replace each $\sin^{-2}\theta$ term by $[-\ln\psi]''$, and we can rewrite (27) and (28) as

$$
\begin{aligned}
\Sigma^+ &= -\frac{8g^2\alpha'^{2-D/2}}{(8\pi^2)^{D/2}}\int_0^1 \frac{dq}{q}\left(\frac{-\pi}{\ln q}\right)^{(10-D)/2} P_+(q) \\
&\int_0^\pi d\theta\bigg((-\psi^2(\theta)[\ln\psi]'')^{\alpha' t}\frac{\alpha' t}{[\ln\psi]''}X^+ - \frac{1}{4}[(-\psi^2(\theta)[\ln\psi]'')^{\alpha' t} - 1][-\ln\psi]''\bigg) \qquad (33) \\
\Sigma^- &= -\frac{8g^2\alpha'^{2-D/2}}{(8\pi^2)^{D/2}}\int_0^1 \frac{dq}{q}\left(\frac{-\pi}{\ln q}\right)^{(10-D)/2} P_-(q) \\
&\int_0^\pi d\theta\bigg((-\psi^2(\theta)[\ln\psi]'')^{\alpha' t}\frac{\alpha' t}{[\ln\psi]''}X^- - \frac{1}{4}[(-\psi^2(\theta)[\ln\psi]'')^{\alpha' t} - 1][-\ln\psi]''\bigg) \qquad (34)
\end{aligned}
$$

Written this way $\Sigma^\pm$ formally vanish as $t \to 0$, which is expected since the massless open string state is a gauge particle and should remain massless. The corrected Regge trajectory is

$$
\alpha(t) = 1 + \alpha' t + \frac{1}{2}(\Sigma^+ - \Sigma^-) \equiv 1 + \alpha' t + \Sigma(t) \qquad (35)
$$

As we have already mentioned $\Sigma(t)$ formally vanishes at $t = 0$. We shall see in the next section that, because of the possibility of infrared divergences when $D \leq 4$, $\Sigma(0)$ is actually zero only when $D > 4$.

4 Small t behavior of $\Sigma(t)$ and the Field Theory Limit

The field theory limit of string theory is controlled by the zero slope limit $\alpha' \to 0$. In open string theory, this entails analyzing the behavior of physical quantities at low momentum $\alpha' k_l \cdot k_m \ll 1$. In this section, we wish to study the small t behavior of the open string Regge trajectory. The one loop correction to this trajectory should reflect the one-loop Reggeization of the gluon in gauge theory.

The part of $\Sigma(t)$ analytic in t (i.e. integer powers) receives contributions from the whole range of q, but non-analytic behavior in Σ at $t=0$ is produced by integration of q near 1. Thus it is convenient in this section to transform to the w variables $\ln w = 2\pi^2/\ln q = -2\pi i/\tau$, via the Jacobi imaginary transformation, and our focus will be on the small w contribution to Σ. For the reader's convenience we have listed the needed Jacobi transforms, as well as some useful identities in the appendix.

The measure change is $q^{-1}dq \to 2\pi^2(w\ln^2 w)^{-1}dw$, from which we find the small w behavior

$$\left(\frac{-\pi}{\ln q}\right)^{5-D/2}\frac{dq}{q}\frac{P_+ + P_-}{2} \quad \sim \quad \frac{dw}{2w}\left(\frac{-2\pi}{\ln w}\right)^{1+D/2} w^{-1/2} \tag{36}$$

$$\left(\frac{-\pi}{\ln q}\right)^{5-D/2}\frac{dq}{q}\frac{P_+ - P_-}{2} \quad \sim \quad (D+S-2)\frac{dw}{2w}\left(\frac{-2\pi}{\ln w}\right)^{1+D/2} . \tag{37}$$

X^+ and X^- enter the integrand of $\Sigma_+ - \Sigma_-$ in the combination

$$\left(\frac{-\pi}{\ln q}\right)^{5-D/2}\frac{dq}{q}(P_+X^+ - P_-X^-) \quad \sim \quad \frac{dw}{w}\left(\frac{-2\pi}{\ln w}\right)^{-3+D/2}\left[4 + \frac{D+S-2}{\pi^2}\left(\frac{2\pi}{\ln w}\right)^2\right] \tag{38}$$

Thus the contribution of the small w region to the correction to the Regge trajectory, which can produce nonanalytic behavior as $t \to 0$, is

$$\begin{aligned}\Sigma_\delta \quad \approx \quad & -\frac{8g^2\alpha'^{2-D/2}}{(8\pi^2)^{D/2}}\int_0^\delta \frac{dw}{w}\left(\frac{-2\pi}{\ln w}\right)^{-3+D/2}\int_0^\pi d\theta\Bigg((-\psi^2(\theta)[\ln\psi]'')^{\alpha' t}\frac{\alpha' t}{[\ln\psi]''}\left[2 + \frac{D+S-2}{2\pi^2}\left(\frac{2\pi}{\ln w}\right)^2\right] \\ & -\frac{D+S-2}{8}\left(\frac{2\pi}{\ln w}\right)^4[(-\psi^2(\theta)[\ln\psi]'')^{\alpha' t} - 1][-\ln\psi]''\Bigg) .\end{aligned} \tag{39}$$

To discuss the small t behavior of $\Sigma(t)$, we examine the t dependent factor of the small w integrand. We set $w = e^{-T}$ and $\theta = \pi x$, and note that at large $T > e^{1/\delta}$

$$-\psi^2(\theta)[\ln\psi]'' \quad \sim \quad e^{x(1-x)T}(1-e^{-xT})^2(1-e^{-(1-x)T})^2\left[\frac{1}{T} + \frac{e^{-xT}}{(1-e^{-xT})^2} + \frac{e^{-(1-x)T}}{(1-e^{-(1-x)T})^2}\right] . \tag{40}$$

This quantity is raised to the power $\alpha' t = -\alpha'|t|$ since we limit ourselves to $t < 0$, where the integral representation of Σ is valid. The factor $e^{-x(1-x)T\alpha'|t|}$ limits the quantity $x(1-x)T < 1/\alpha'|t|$. Nonanalytic behavior in t as $t \to 0$ can be produced by integration over the region $1 \ll \Lambda < x(1-x)T < \infty$. In this region $w^{\theta/\pi} = e^{-xT} \ll 1$ and $w^{1-\theta/\pi} = e^{-(1-x)T} \ll 1$, so the t dependent factor in the integrand reduces to

$$(-\psi^2(\theta)[\ln\psi]'')^{-\alpha'|t|} \quad \sim \quad T^{\alpha'|t|}e^{-x(1-x)T\alpha'|t|} \tag{41}$$

Then the small w (or large T) contribution to Σ simplifies to

$$\begin{aligned}\Sigma_\delta \quad \approx \quad & -\frac{8g^2\alpha'^{2-D/2}}{(8\pi^2)^{D/2}}\int_{\Lambda/x(1-x)}^\infty dT\left(\frac{2\pi}{T}\right)^{-2+D/2}\int_0^1 \pi dx\Bigg(-\pi\alpha' t T^{\alpha'|t|}e^{-x(1-x)T\alpha'|t|} \\ & -\frac{D+S-2}{4\pi}\left(\frac{2\pi}{T}\right)^2\left[T^{\alpha'|t|}e^{-x(1-x)T\alpha'|t|} - 1\right]\Bigg) \\ \approx \quad & -\frac{8g^2\alpha'^{2-D/2}}{(4\pi)^{D/2}}\Bigg(\frac{-\alpha' t}{4}\frac{\Gamma(-2+\alpha' t + D/2)^2}{\Gamma(D-4+2\alpha' t)}\int_\Lambda^\infty du\, u^{2-\alpha' t - D/2}e^{-u\alpha'|t|} \\ & -\frac{D+S-2}{4}\int_\Lambda^\infty du\, u^{-D/2}\left[\frac{\Gamma(\alpha' t + D/2)^2}{\Gamma(D+2\alpha' t)}u^{-\alpha' t}e^{-u\alpha'|t|} - \frac{\Gamma(D/2)^2}{\Gamma(D)}\right]\Bigg) .\end{aligned} \tag{42}$$

The first integral is of the form (putting $\xi = \alpha'|t| = -\alpha' t$)

$$\int_\Lambda^\infty du u^a e^{-u\xi} \;=\; \xi^{-a-1}\int_{\xi\Lambda}^\infty du u^a e^{-u} \sim \xi^{-a-1}\Gamma(a+1), \qquad a+1>0. \tag{43}$$

If $a+1 \leq 0$, a few integration by parts shows that

$$\int_\Lambda^\infty du u^a e^{-u\xi} \;=\; \xi^{-a-1}\int_{\xi\Lambda}^\infty du u^a e^{-u} \sim \xi^{-a-1}\Gamma(a+1) + \mathcal{P}(\xi,\Lambda)e^{-\xi\Lambda}\,, \tag{44}$$

where $\mathcal{P}$ is a polynomial in ξ (and hence a polynomial in t) with Λ dependent coefficients. In the expression for Σ the term involving $\mathcal{P}$ is multiplied by a function analytic at $t=0$ and so contributes integer powers of t to Σ. Thus the nonanalytic fractional power, though always present, dominates the behavior only if $a+1>0$. For the first integral this means $D<6$.

The subtraction term in the second integral is finite provided $D>2$, which is not a serious restriction. The analysis of that integral again leads to an expression of the form (44), with the subtraction term simply cancelling the constant term in the power series arising from $\mathcal{P}(\xi,\Lambda)$. Collecting the results for both integrals we find the small t behavior

$$\begin{aligned}\Sigma \;&\sim\; -\frac{2g^2\alpha'^{2-D/2}}{(4\pi)^{D/2}}\biggl(\frac{\Gamma(-2+\alpha't+D/2)^2}{\Gamma(D-4+2\alpha't)}(-\alpha't)^{\alpha't-2+D/2}\Gamma(3-\alpha't-D/2)\\ &\qquad -(D+S-2)\frac{\Gamma(\alpha't+D/2)^2}{\Gamma(D+2\alpha't)}(-\alpha't)^{\alpha't-1+D/2}\Gamma(1-\alpha't-D/2)\biggr)+O(\alpha't) \qquad (45)\\ &\sim\; -\frac{2g^2\alpha'^{2-D/2}}{(4\pi)^{D/2}}\frac{\Gamma(-2+D/2)^2}{\Gamma(D-4)}(-\alpha't)^{-2+D/2}\Gamma(3-D/2)+O(\alpha't\ln(-\alpha't))\,. \qquad (46)\end{aligned}$$

In the first line, we show the second term proportional to $(D+S-2)$, which is down by a factor of $\alpha't$ compared to the first term to stress that the number of massless scalars S does not figure in the leading small t behavior. With the $O(\alpha't\ln(-\alpha't))$ term we stress that the displayed first term is dominant only for $D<6$, and when $D>6$ it is only significant when $D/2$ is not an integer. The contributions to Σ from w away from zero by a finite amount are analytic in t, i.e. a series of integer powers of t starting with the first power, since $\Sigma(0)=0$. To properly regulate infrared divergences (which would, among other things, invalidate the integral representation for Σ), we would also need to stipulate that $D>4$, so in practice this formula gives the dominant small t behavior only in the range $4<D<6$.

The leading small t behavior $(-\alpha't)^{(D-4)/2}$ we have demonstrated is precisely that of a D-dimensional gauge theory: the one loop correction of which is consistent with Regge behavior with a trajectory $\alpha(t) = 1 + C(-t/\mu^2)^{(D-4)/2}$. As $D\to 4$ from above the pole at $D=4$ shows that a $\ln(-\alpha't)$ dependence remains:

$$\Sigma_{D\to 4} \sim -\frac{g^2}{4\pi^2}\left[\frac{2}{D-4}+\ln(-\alpha't)\right] \tag{47}$$

Consulting known results for one loop gauge theory diagrams [26], as explained and developed in [8, 9, 27], we find that the small t behavior of the open string trajectory agrees exactly with that inferred from conventional one loop gauge theory calculations.

5 Large t Behavior of $\Sigma(t)$

The large t behavior of the trajectory function is dominated by the small q region. Thus it is more convenient to write the integral in this variable. Combining equations (33) and (34) we have

$$\begin{aligned}\Sigma(t) \;=\; -\frac{4g^2\alpha'^{2-D/2}}{(8\pi^2)^{D/2}}\int_0^1\frac{dq}{q}\left(\frac{-\pi}{\ln q}\right)^{(10-D)/2}\int_0^\pi d\theta\,\biggl((-\psi^2(\theta)[\ln\psi]'')^{\alpha't}\frac{\alpha't}{[\ln\psi]''}(P_+X^+-P_-X^-)\\ -\frac{1}{4}(P_+-P_-)\Bigl[(-\psi^2(\theta)[\ln\psi]'')^{\alpha't}-1\Bigr][-\ln\psi]''\biggr) \qquad (48)\end{aligned}$$

For later convenience, we write the partition functions as

$$
\begin{aligned}
P_+ &= 16(1-w^{1/2})^{10-D-S}\frac{\theta_3(0)^4}{\theta_1'(0)^4} \\
P_- &= 16(1+w^{1/2})^{10-D-S}\frac{\theta_2(0)^4}{\theta_1'(0)^4}
\end{aligned}
\tag{49}
$$

where we have used the fact that

$$
\frac{\prod_r^\infty (1+q^{2r})^8}{\prod_n^\infty (1-q^{2n})^8} = 16q\frac{\theta_3(0)^4}{\theta_1'(0)^4} \quad , \quad \frac{\prod_n^\infty (1+q^{2n})^8}{\prod_n^\infty (1-q^{2n})^8} = 16q\frac{\theta_2(0)^4}{\theta_1'(0)^4}
\tag{50}
$$

Expanding about $q=0$ we have:

$$
P_+ - P_- \simeq P_+ \simeq q^{-1}\left(\frac{-\pi^2}{\ln q}\right)^{10-D-S} \tag{51}
$$

$$
P_+X^+ - P_-X^- \simeq 4\left(\frac{-\pi^2}{\ln q}\right)^{10-D-S} \tag{52}
$$

$$
[-\ln\psi]'' = \csc^2\theta + \mathcal{O}(q^2) \tag{53}
$$

$$
\log(-\psi^2(\log\psi)'') = 16q^2\sin^4\theta + \mathcal{O}(q^4) \tag{54}
$$

The small q contribution to the trajectory function (48) becomes

$$
\begin{aligned}
\Sigma(t) \simeq\ & \frac{16g^2\alpha'^{2-D/2}}{(8\pi^2)^{D/2}}\alpha' t\int_0^\delta \frac{dq}{q}\left(\frac{-\pi}{\ln q}\right)^{25-5D/2-2S}\int_0^\pi d\theta\, e^{-\alpha'|t|16q^2\sin^4\theta}\sin^2\theta \\
&+\frac{g^2\alpha'^{2-D/2}}{(8\pi^2)^{D/2}}\int_0^\delta \frac{dq}{q^2}\left(\frac{-\pi}{\ln q}\right)^{25-5D/2-2S}\int_0^\pi d\theta\left[e^{-\alpha'|t|16q^2\sin^4\theta}-1\right]\csc^2\theta
\end{aligned}
\tag{55}
$$

Although the presence of the explicit factor of t in front of the first integral above makes this term the dominant one, a careful analysis shows that this term is larger than the second one by a factor of $\sqrt{t}$, not by a factor of t. Therefore we study the expression

$$
I \equiv \int_0^\delta \frac{dq}{q}\left(\frac{-1}{\ln q}\right)^a\int_0^\pi d\theta\,\sin^2\theta\, e^{-16q^2|\alpha' t|\sin^4\theta} \tag{56}
$$

in the limit $|\alpha' t|\to\infty$ where $a\equiv 25-5D/2-2S$. Performing the change of variable $u=-\ln q$ we have

$$
I \equiv \int_{-\ln\delta}^\infty du\left(\frac{1}{u}\right)^a\int_0^\pi d\theta\,\sin^2\theta\,\exp\left[-\exp\left[\ln(16|\alpha' t|\sin^4\theta)-2u\right]\right] \tag{57}
$$

followed by the change $u=\xi\ln(16\alpha'|t|\sin^4\theta)$, yields

$$
I \equiv \int_0^\pi d\theta\,\sin^2\theta f(\theta)^{1-a}\int_{\ln\delta/f(\theta)}^\infty d\xi\,\xi^{-a}\exp\left[-\exp\left[(1-2\xi)f(\theta)\right]\right] \tag{58}
$$

where $f(\theta)\equiv\ln(16\alpha'|t|\sin^4\theta)$. At fixed θ, the exponential factor restricts the integration over ξ to the range $1/2<\xi<\infty$ as $|t|\to\infty$, and since there are no singularities coming from the end points of the θ integration we have

$$
I \simeq \left(\frac{1}{\ln|\alpha' t|}\right)^{a-1}\int_0^\pi d\theta\,\sin^2\theta\int_{1/2}^\infty d\xi\,\xi^{-a} \tag{59}
$$

$$
\simeq \frac{\pi}{2}\left(\frac{1}{\ln|\alpha' t|}\right)^{a-1}\frac{2^{a-1}}{a-1} \tag{60}
$$

Putting this result into (55) we finally have

$$\Sigma(t) \;\simeq\; g^2\alpha' \frac{(8\pi^2\alpha')^{1-D/2}}{24-5D/2-2S}\alpha' t\left(\frac{2\pi}{\ln|\alpha' t|}\right)^{24-5D/2-2S} \tag{61}$$

as $|t| \to \infty$.

6 Numerical Calculations and Graphics

We present here a numerical analysis of the trajectory function $\Sigma(t)$ in both limits studied, large t and small t as well as in the full range between these two asymptotic regions. We will see that the numerical computation of the integral representation of the trajectory function $\Sigma(t)$ matches well with the asymptotic analytical predictions described in sections 4 and 5.

At large t we expect $\Sigma(t)$ to behave like (61). As a numerical example, let us consider the case when there is the maximum number of scalars circulating in the loop $S = 10 - D$, in $D = 5$ i.e. open strings ending on a D4-brane. We expect at large t:

$$\Sigma(t)_{lead} \;\simeq\; \lambda\alpha' t\frac{4\pi^2}{3}\left(\frac{2\pi}{\ln|\alpha' t|}\right)^{3/2} \tag{62}$$

where $\lambda \equiv 4g^2\alpha'^{2-D/2}/(8\pi^2)^{D/2}$. For plotting convenience, we show in Figure 1 both the numerical evaluation of $\Sigma(t)/\lambda\alpha' t$ directly from equation (48) represented by the dots, and we show the leading estimate

$$\frac{\Sigma(t)_{lead}}{\lambda\,\alpha' t} \sim \frac{4\pi^2}{3}\left(\frac{2\pi}{\ln|\alpha' t|}\right)^{3/2} \tag{63}$$

by the solid line. From the figure we see that the numerical evaluation of the full trajectory function (48) approaches the predicted behavior at large $|t|$, although the approach is very slow due to the logarithmic dependence. Due to computational limitations of the integration routine, the maximum value of $-\alpha' t$

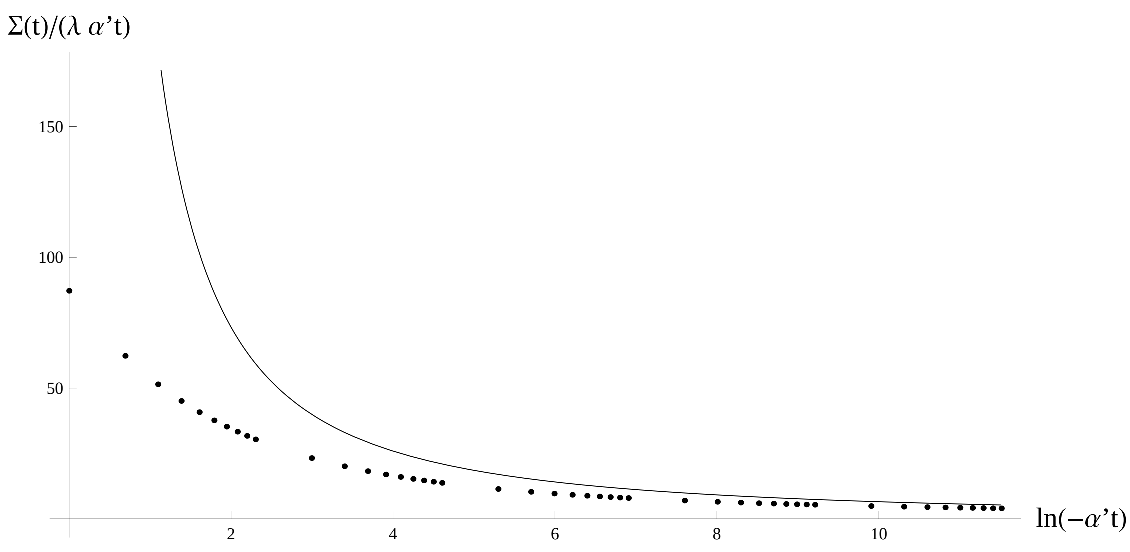

Figure 1: The dots correspond to the direct numerical integration of $\Sigma(t)/(\lambda t)$ while the solid line is the predicted behavior at large $|t|$ both as a function of $\ln(-\alpha' t)$. At large values of $\alpha'|t|$ the numerical integration approaches the predicted behavior from below.

for which the trajectory function could be numerically evaluated was of the order of $-\alpha' t \sim 10^5$ which corresponds to the upper limit $\ln(10^5) \sim 11.5$ in the horizontal axis shown in the figures. Performing a fit of the exact numerical evaluation using the leading and the next three subleading corrections we obtain

$$\frac{\Sigma}{\lambda\,\alpha' t} \sim 12.89\left(\frac{2\pi}{\ln|\alpha' t|}\right)^{3/2} - 7.74\left(\frac{2\pi}{\ln|\alpha' t|}\right)^{5/2} + 4.84\left(\frac{2\pi}{\ln|\alpha' t|}\right)^{7/2} - 0.85\left(\frac{2\pi}{\ln|\alpha' t|}\right)^{9/2} \tag{64}$$

whose leading term is to be compared with the predicted leading behavior

$$\frac{\Sigma(t)_{lead}}{\lambda\,\alpha' t} \sim \frac{4\pi^2}{3}\left(\frac{2\pi}{\ln|\alpha' t|}\right)^{3/2} \sim 13.16\left(\frac{2\pi}{\ln|\alpha' t|}\right)^{3/2} \tag{65}$$

which is in good agreement with the analytic prediction. Figure 2 shows the fitting function (64) together with the data points.

Now we turn to the small t behavior. As has been noted in section 3, this is best studied in the w variables

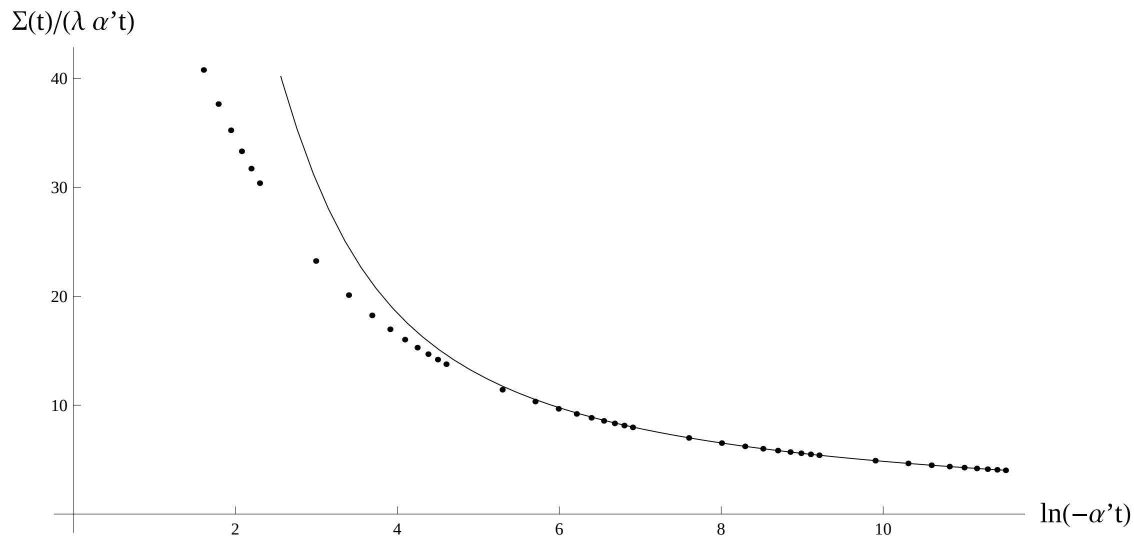

Figure 2: The fit of the leading and three subleading corrections to the data points is presented as the solid line. Here we see that the agreement between the data points and the fit increases for larger values of $\alpha' t$ as expected, and it is already good starting at $\ln(\alpha' t) \sim 6$ since we have included subleading corrections.

since it is the $w \sim 0$ region that dominates the nonanalytic behavior at small t. We need the exact form of $\Sigma(t)$ which, using the integral representation as a function of w is:

$$\begin{aligned}\Sigma(t) \;=\; \lambda \int_0^1 \frac{dw}{2w}\left(\frac{-2\pi}{\ln w}\right)^{-3+D/2} \int_0^\pi d\theta\, \Bigg((-\psi^2(\theta)[\ln\psi]'')^{\alpha' t}\frac{\alpha' t}{[\ln\psi]''}(P_+X^+ - P_-X^-) \\ -\frac{1}{4}(P_+ - P_-)\left[(-\psi^2(\theta)[\ln\psi]'')^{\alpha' t} - 1\right][-\ln\psi]''\Bigg)\end{aligned} \tag{66}$$

To evaluate it numerically we need the exact w-dependent forms of the expressions listed in section 4, the partition functions in (49), and also:

$$[-\ln\psi]'' = \left(\frac{\ln w}{2\pi}\right)^2 \theta_3^2(0,\sqrt{w})\theta_2^2(0,\sqrt{w})\frac{\theta_4^2(i\theta\ln w/2\pi,\sqrt{w})}{\theta_1^2(i\theta\ln w/2\pi,\sqrt{w})} - \frac{2\mathbf{E}}{\pi}\left(\frac{-\ln w}{2\pi}\right)\theta_3^2(0,\sqrt{w}) \tag{67}$$

The numerical integration routine produces the plot in Figure 3 for the range $\alpha' t \in [-1, -0.01]$ which suggests that $\Sigma(t)$ approaches zero with infinite slope as it should reading off from (46). Nonetheless, we would like to see whether the numerics is really producing this behavior at small t. In order to do this, we need to zoom in near zero in Figure 3 in which case we do the following: we separate out the small w region as

$$\int_0^1 dq[\cdots] = \int_0^{q_0} dq[\cdots] + \int_0^{w_0} dw[\cdots] \tag{68}$$

If for instance, we take $q_0 = 0.8$, by means of $w = e^{2\pi^2/\ln q}$ we see that the upper limit in the w integration

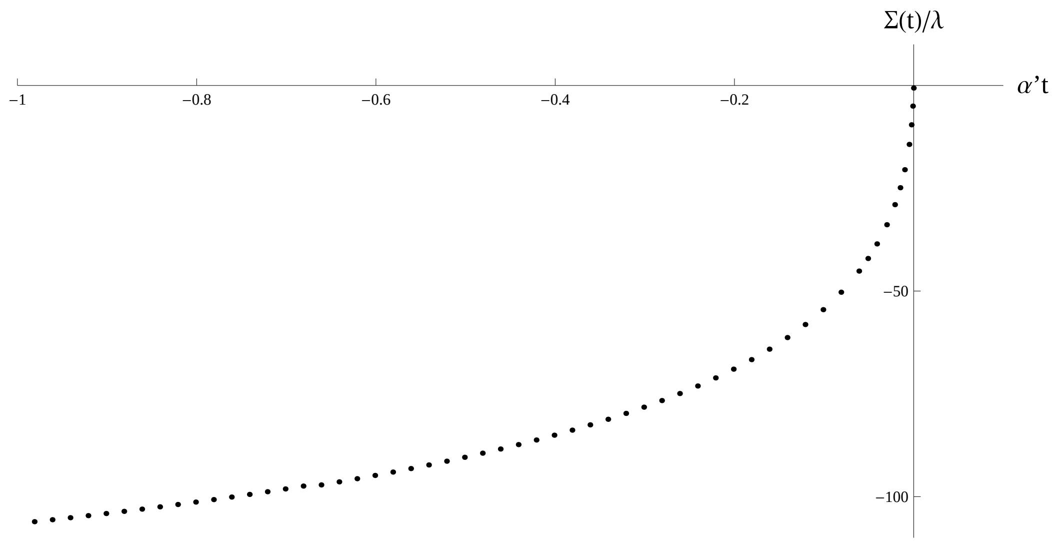

Figure 3: The small t behavior is shown for $D = 5$. We expect $\Sigma(t)$ to go to zero with infinite slope which can be appreciated from this figure.

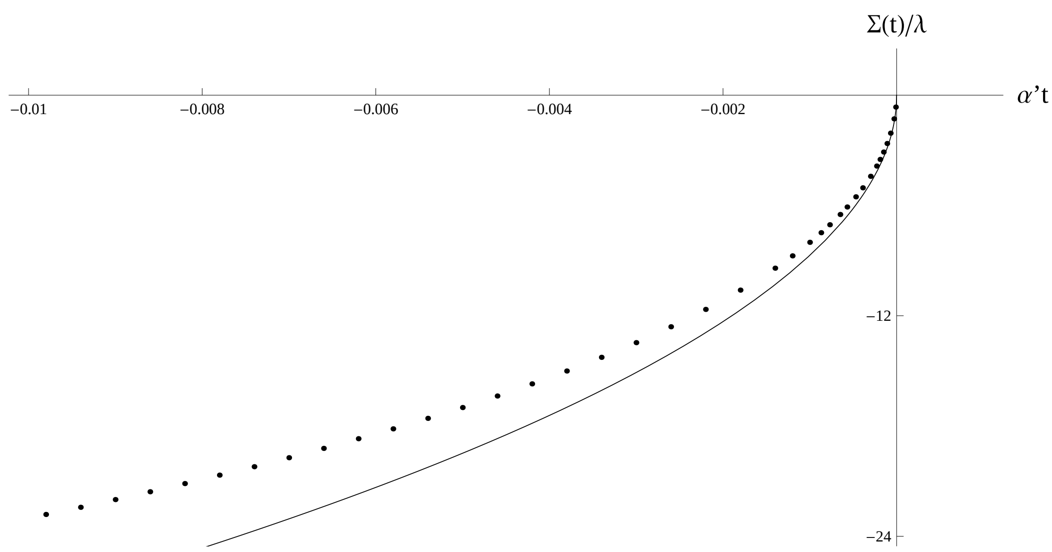

Figure 4: Zoom in small t. The expected $\Sigma \sim (-\alpha' t)^{1/2}$ behavior near $t = 0$ can be appreciated more clearly in this figure. The solid line is the predicted asymptotic behavior $\Sigma(t)/\lambda \sim -2^{3/2}\pi^4(-\alpha' t)^{1/2}$ as $t \to 0$ which matches well with the data points in this limit.

is $w_0 \sim 4 \times 10^{-39}$ which is very small and allows one to use the asymptotic expression (39) with ψ and

$[-\ln\psi]''$ being also approximated by:

$$\psi \simeq \frac{\pi}{T} e^{x/2(1-x)T}(1-e^{-xT})(1-e^{-(1-x)T}) \tag{69}$$

$$[-\ln\psi]'' \simeq \frac{1}{\pi^2}\left[T + T^2\left(\frac{e^{-xT}}{(1-e^{-xT})^2} + \frac{e^{-(1-x)T}}{(1-e^{-(1-x)T})^2}\right)\right] \tag{70}$$

as shown in equation (40). The numerical evaluation of (39) in this case is shown in Figure 4. A fit of the data points including the leading and subleading powers turns out to be

$$\frac{\Sigma}{\lambda} \sim -262.82(-\alpha' t)^{1/2} - 323.26\,\alpha' t \tag{71}$$

The analytic expression for the leading behavior is given by (46) which in this case becomes

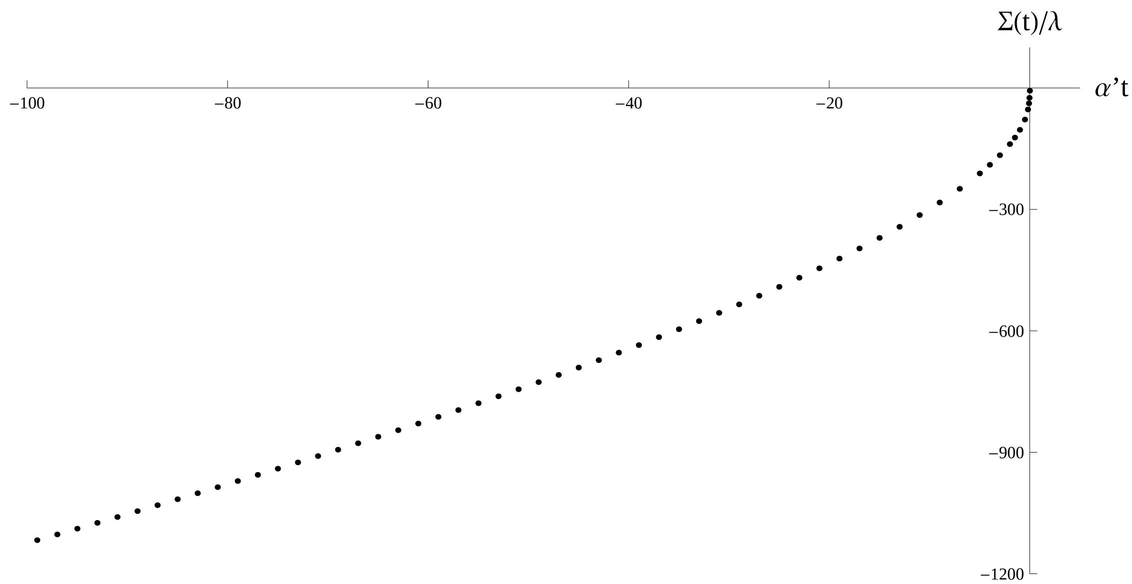

Figure 5: A larger range that includes both large and small t behavior is shown. In this plot it is possible to see the two asymptotic regions with some accuracy. The large t region grows as $\sim t/(\ln t)^{3/2}$ as described in Section 5. Although it is not completely evident from this figure, $\Sigma(t)$ is going to zero with infinite slope as $(-\alpha' t)^{1/2}$ in the region near $t = 0$ (see Figure 4)

$$\frac{\Sigma}{\lambda} \sim -\frac{(2\pi)^{D/2}}{2}\frac{\Gamma(-2+D/2)^2}{\Gamma(D-4)}(-\alpha' t)^{D/2-2}\Gamma(3-D/2) \sim -2^{3/2}\pi^4(-\alpha' t)^{1/2} \tag{72}$$

for $D = 5$. From here we see that we have good agreement with (71) since $2^{3/2}\pi^4 = 275.52$. We finish this section by showing a larger range in t in which the two asymptotic regions $t \sim 0$ and $t \to -\infty$ can be visualized. Although it is not evident from the plot, Figure 5 shows the two asymptotic regions we have described above i.e., $\Sigma \sim (-\alpha' t)^{1/2}$ as $t \to 0$ and $\Sigma \sim \alpha' t/(\ln|\alpha' t|)^{3/2}$ as $t \to -\infty$.

7 Discussion and Conclusions

In this paper we have understood one more aspect about the relation between the dynamics of open strings and their corresponding gauge field theory limit, namely we have extracted the leading Regge trajectory $\alpha(t) = 1 + \alpha' t + \Sigma(t)$ of open strings ending on a stack of N Dp-branes including the planar one-loop corrections. When studying the $t \to 0$ limit, besides confirming that the correction goes to zero as a reflection of the masslessness of the open string gluon, we have also shown that it behaves as $\Sigma \sim -Cg^2(\alpha' t)^{(D-4)/2}/(D-4)$ which is precisely the result obtained in D dimensional gauge theory. In the $D \to 4$ case, which corresponds to a D3-brane where the dynamics of the open strings describe the 4-dimensional $SU(N)$ gauge-theory in 't Hooft's planar limit, the $t \to 0$ limit of $\Sigma(t)$ is

$$\Sigma_{D\to 4} \sim -\frac{g^2}{4\pi^2}\left[\frac{2}{D-4} + \ln(-\alpha' t)\right] \tag{73}$$

which precisely matches the results known from one-loop gauge theory calculations. We have also studied the limit $t \to -\infty$ of $\Sigma(t)$ where we obtained:

$$\Sigma(t) \simeq g^2\alpha' \frac{(8\pi^2\alpha')^{1-D/2}}{24-5D/2-2S}\alpha' t \left(\frac{2\pi}{\ln|\alpha' t|}\right)^{24-5D/2-2S} \tag{74}$$

Since the maximum number of scalars circulating in the loop is $S_{\max} = 10 - D$ the 1-loop correction stays smaller than the tree trajectory for arbitrarily large $-\alpha' t$ as long as $D < 8$.

We have seen once again the usefulness of the GNS regulator[7] when dealing with the "spurious" divergences encountered in the integration over θ. The subtraction (31) is very simple, and it is actually zero after analytic continuation to $P = 0$.

When we organized the integrand in the form of equations (33) and (34), the recognition that the quantities $X^{\pm}$ defined in (75) and (76) were independent of the integration variable θ significantly improved the numerical calculations performed in Section 7.

There is still much work to be done. We are pursuing the idea that some aspects of QCD both perturbative and nonperturbative (such as confinement as an example of the latter) could be more tractable in the open string theory that has (large N) QCD as its low energy limit rather than in the field theory itself. One of the simplest open string theories that satisfies this requirement, and the one that we used in this article, is the even G-Parity sector of the Neveu-Schwarz model in 10 dimensions with the odd G-Parity states projected out to have a tachyon free spectrum. The end points of the open strings are required to be attached to a stack of N Dp-branes as is customary. Since QCD does not contain massless scalars, we also prevent them from circulating in the loop by projecting them out using the proposal in [17]. However, our calculations also apply for Yang-Mills theories with massless scalars by simply choosing different values of the number of massless scalars S in equations (33) and (34) as long as $0 \leq S \leq 10 - D$ where D is the space-time dimensionality of the Dp-brane.

Summarizing, we expect to learn much more from this model in the near future. One immediate and straightforward follow-up to this work would be to repeat the analysis in the cases where the open strings end on D7 and D8 branes to encompass these two extra cases as well. In these cases there are extra subleading divergences that need to be taken care of (due to the emission of massless closed string states into the vacuum) which however can be absorbed into a renormalization of the Regge slope parameter α'. Further studies of this model, such as an explicit expression free of spurious divergences for the complete 1-loop planar M-gluon amplitude, and the comparison of the low energy limits of these string amplitudes to the limiting field theory calculations are tasks for the immediate future. We regard this work to be a further step in setting up the calculation for the complete sum of planar open string multiloop diagrams, which we hope will shed light on nonperturbative issues of gauge theory.

A Elliptic Functions and Jacobi Transformations

We begin by giving the dramatic simplification of $X^{\pm}$:

$$X^+(\theta) \quad = \quad \frac{1}{4}\theta_4(0)^4\theta_3(0)^4 - \frac{\boldsymbol{E}}{\pi}\theta_4(0)^4\theta_3(0)^2 + \frac{\boldsymbol{E}^2}{\pi^2}\theta_3(0)^4 = 4q + O(q^2) \tag{75}$$

[7] See Appendix A in [22] for an application of this regulator in conventional field theory.

$$X^-(\theta) = -\frac{1}{4}\theta_4(0)^4\theta_3(0)^4 + \frac{\boldsymbol{E}^2}{\pi^2}\theta_3(0)^4 = O(q^2) \tag{76}$$

$$\boldsymbol{E} = \frac{\pi}{6\theta_3(0)^2}\left(\theta_3(0)^4 + \theta_4(0)^4 - \frac{\theta_1'''(0)}{\theta_1'(0)}\right) = \frac{\pi}{2} - 2\pi q + O(q^2) \tag{77}$$

where we have shown on the extreme right of each equation its small q behavior. Remarkably, $X^\pm$ turn out to be independent of θ! The most efficient way to show this is to express $\chi_\pm$ and $-[\ln\psi]''$ in terms of the Jacobian elliptic functions sn, cn, and dn. Then one exploits the many identities these functions and their derivatives satisfy [25].

The following expansions are useful:

$$\theta_3(0) = \prod_n (1-q^{2n})\prod_r (1+q^{2r})^2 \tag{78}$$

$$\theta_4(0) = \prod_n (1-q^{2n})\prod_r (1-q^{2r})^2 \tag{79}$$

$$\frac{\theta_1'''(0)}{\theta_1'(0)} = -1 + 24\sum_n \frac{q^{2n}}{(1-q^{2n})^2} \tag{80}$$

where sums over n are over positive integers and those over r are over half odd integers.

Next we list the Jacobi transforms of the various quantities we have introduced in this paper. The partition functions change according to

$$P_+ \equiv q^{-1}(1-w^{1/2})^{10-D-S}\frac{\prod_r(1+q^{2r})^8}{\prod_n(1-q^{2n})^8} = \left(\frac{2\pi}{\ln w}\right)^4 w^{-1/2}(1-w^{1/2})^{10-D-S}\frac{\prod_r(1+w^r)^8}{\prod_n(1-w^n)^8} \tag{81}$$

$$P_- \equiv 2^4(1+w^{1/2})^{10-D-S}\frac{\prod_n(1+q^{2n})^8}{\prod_n(1-q^{2n})^8} = \left(\frac{2\pi}{\ln w}\right)^4 w^{-1/2}(1+w^{1/2})^{10-D-S}\frac{\prod_r(1-w^r)^8}{\prod_n(1-w^n)^8} \tag{82}$$

Next we turn to the Jacobi transforms of the θ dependent factors.

$$\theta_1\left(\frac{i\theta\ln w}{2\pi},\sqrt{w}\right) = -i\left(\frac{-2\pi}{\ln w}\right)^{1/2}\exp\left\{\frac{-\theta^2\ln w}{2\pi^2}\right\}\theta_1(\theta,q) \tag{83}$$

$$\theta_1'(0,\sqrt{w}) = \left(\frac{-2\pi}{\ln w}\right)^{3/2}\theta_1'(0,q) \tag{84}$$

$$\begin{aligned}\psi(\theta,q) &= \frac{\theta_1(\theta,q)}{\theta'(0)} = i\frac{-2\pi}{\ln w}\exp\left\{\frac{\theta^2\ln w}{2\pi^2}\right\}\frac{\theta_1\left(i\theta\ln w/2\pi,\sqrt{w}\right)}{\theta_1'(0,\sqrt{w})}\\ &= \frac{\pi}{-\ln w}\exp\left\{-\frac{\theta(\pi-\theta)\ln w}{2\pi^2}\right\}(1-w^{\theta/\pi})(1-w^{1-\theta/\pi})\\ &\qquad \prod_{n=1}^{\infty}\frac{(1-w^{n+\theta/\pi})(1-w^{n+1-\theta/\pi})}{(1-w^n)^2}\end{aligned} \tag{85}$$

$$-\frac{\partial^2}{\partial\theta^2}\ln\psi = \frac{-\ln w}{\pi^2} + \frac{\ln^2 w}{\pi^2}\sum_{n=0}^{\infty}\left[\frac{w^{n+\theta/\pi}}{(1-w^{n+\theta/\pi})^2} + \frac{w^{n+1-\theta/\pi}}{(1-w^{n+1-\theta/\pi})^2}\right] \tag{86}$$

We have written ψ and its double logarithmic derivative in a way that is manifestly symmetric under $\theta\to\pi-\theta$. Continuing with our list of Jacobi transforms,

$$\boldsymbol{E} = \frac{-\ln w}{12\theta_3^2(0,\sqrt{w})}\left(\theta_3^4(0,\sqrt{w}) + \theta_2^4(0,\sqrt{w}) + \frac{\theta_1'''(0.\sqrt{w})}{\theta_1'(0,\sqrt{w})} - \frac{12}{\ln w}\right) \tag{87}$$

$$X^+ = \left(-\frac{\ln w}{2\pi}\right)^4\frac{\theta_3^4(0,\sqrt{w})\theta_2^4(0,\sqrt{w})}{4} - \frac{\boldsymbol{E}}{\pi}\left(-\frac{\ln w}{2\pi}\right)^3\frac{\theta_3^2(0,\sqrt{w})\theta_2^4(0,\sqrt{w})}{4}$$

$$+\frac{\boldsymbol{E}^2}{\pi^2}\left(-\frac{\ln w}{2\pi}\right)^2\theta_3^4(0,\sqrt{w}) \tag{88}$$

$$X^- = -\left(-\frac{\ln w}{2\pi}\right)^4\frac{\theta_3^4(0,\sqrt{w})\theta_2^4(0,\sqrt{w})}{4}+\frac{\boldsymbol{E}^2}{\pi^2}\left(-\frac{\ln w}{2\pi}\right)^2\theta_3^4(0,\sqrt{w}) \tag{89}$$

$$X^+ - X^- = 2\left(-\frac{\ln w}{2\pi}\right)^4\frac{\theta_3^4(0,\sqrt{w})\theta_2^4(0,\sqrt{w})}{4}-\frac{\boldsymbol{E}}{\pi}\left(-\frac{\ln w}{2\pi}\right)^3\frac{\theta_3^2(0,\sqrt{w})\theta_2^4(0,\sqrt{w})}{4} \tag{90}$$

$$X^+ + X^- = -\frac{\boldsymbol{E}}{\pi}\left(-\frac{\ln w}{2\pi}\right)^3\frac{\theta_3^2(0,\sqrt{w})\theta_2^4(0,\sqrt{w})}{4}+2\frac{\boldsymbol{E}^2}{\pi^2}\left(-\frac{\ln w}{2\pi}\right)^2\theta_3^4(0,\sqrt{w}) \tag{91}$$

Finally we need the small w behavior of these combinations of θ functions:

$$\begin{aligned}
\theta_3(0,\sqrt{w}) &= \prod_n(1-w^n)\prod_r(1+w^r)^2 \sim 1+2w^{1/2}+O(w)\\
\theta_2(0,\sqrt{w}) &= 2w^{1/8}\prod_n(1-w^n)\prod_r(1+w^r)^2 \sim 2w^{1/8}(1+O(w))\\
\frac{\theta_1'''(0,\sqrt{w})}{\theta_1'(0,\sqrt{w})} &= -1+24\sum_n\frac{w^n}{(1-w^n)^2}\sim -1+O(w), \qquad \boldsymbol{E}\sim 1+O(w^{1/2}\ln w)
\end{aligned} \tag{92}$$

$$X^+ - X^- \sim 8w^{1/2}\left(\frac{\ln w}{2\pi}\right)^4\left(1+O\left(\frac{1}{\ln w}\right)\right), \qquad X^+ + X^- \sim \frac{2}{\pi^2}\left(\frac{\ln w}{2\pi}\right)^2(1+O(w^{1/2})) \tag{93}$$

X^+ and X^- enter the integrand of $\Sigma_+ - \Sigma_-$ in the combination

$$P_+X^+ - P_-X^- = (X^+ - X^-)\frac{P_+ + P_-}{2}+(X^+ + X^-)\frac{P_+ - P_-}{2} \tag{94}$$

$$\sim 8w^{1/2}\left(\frac{\ln w}{2\pi}\right)^4\frac{P_+ + P_-}{2}+\frac{2}{\pi^2}\left(\frac{\ln w}{2\pi}\right)^2\frac{P_+ - P_-}{2} \tag{95}$$

$$\left(\frac{-\pi}{\ln q}\right)^{5-D/2}\frac{dq}{q}(P_+X^+ - P_-X^-) \sim \frac{dw}{w}\left(\frac{-2\pi}{\ln w}\right)^{-3+D/2}\left[4+\frac{D+S-2}{\pi^2}\left(\frac{2\pi}{\ln w}\right)^2\right] \tag{96}$$

Acknowledgments: We would like to thank André Neveu for helpful discussions. F.R. thanks Christoph Sachse for helpful discussions and Chris Pankow and Myeonghun Park for assistance with plotting. This research was supported in part by the Department of Energy under Grant No. DE-FG02-97ER-41029.

References

[1] J. Scherk, Nucl. Phys. **B31** (1971) 222-234.

[2] A. Neveu and J. Scherk, Nucl. Phys. B **36** (1972) 155.

[3] J. Maldacena, Adv. Theor. Math. Phys. **2**, 231 (1998) [Int. J. Theor. Phys. **38** (1999) 1113], [arXiv:hep-th/9711200].

[4] G. 't Hooft, *Nucl. Phys.* **B72** (1974) 461.

[5] K. Bardakci and C. B. Thorn, Nucl. Phys. **B626** (2002) 287, hep-th/0110301.

[6] C. B. Thorn, Nucl. Phys. B **637** (2002) 272 [arXiv:hep-th/0203167]; S. Gudmundsson, C. B. Thorn, T. A. Tran, Nucl. Phys. **B649** (2003) 3-38. [hep-th/0209102].

[7] R. Giles and C. B. Thorn, *Phys. Rev.* **D16** (1977) 366.

[8] D. Chakrabarti, J. Qiu and C. B. Thorn, Phys. Rev. D **72** (2005) 065022, arXiv:hep-th/0507280.

[9] D. Chakrabarti, J. Qiu and C. B. Thorn, Phys. Rev. D **74** (2006) 045018 [Erratum-ibid. D **76** (2007) 089901] [arXiv:hep-th/0602026].

[10] S. G. Naculich and H. J. Schnitzer, Nucl. Phys. B **794** (2008) 189 [arXiv:0708.3069 [hep-th]]; R. C. Brower, H. Nastase, H. J. Schnitzer and C. I. Tan, Nucl. Phys. B **814** (2009) 293 [arXiv:0801.3891 [hep-th]].

[11] A. Neveu and J. H. Schwarz, Nucl. Phys. B **31** (1971) 86.

[12] A. Neveu, J. H. Schwarz and C. B. Thorn, Phys. Lett. B **35** (1971) 529.

[13] P. Goddard and R. E. Waltz, Nucl. Phys. B **34** (1971) 99.

[14] R. C. Brower and C. B. Thorn, Nucl. Phys. B **31** (1971) 163.

[15] P. Goddard and C. B. Thorn, Phys. Lett. B **40** (1972) 235.

[16] S. Mandelstam, private communication, April 1971.

[17] C. B. Thorn, Phys. Rev. **D78** (2008) 106008. [arXiv:0809.1085 [hep-th]].

[18] K. Kikkawa, B. Sakita, M. A. Virasoro, Phys. Rev. **184** (1969) 1701-1713.

[19] H. J. Otto, V. N. Pervushin, D. Ebert, Theor. Math. Phys. **35** (1978) 308.

[20] V. Alessandrini, D. Amati, B. Morel, Nuovo Cim. **A7**, 797-823 (1972).

[21] R. R. Metsaev and A. A. Tseytlin, Nucl. Phys. B **298** (1988) 109.

[22] C. B. Thorn, Phys. Rev. **D78** (2008) 085022. [arXiv:0808.0458 [hep-th]].

[23] A. Neveu and J. Scherk, Nucl. Phys. B **36** (1972) 317.

[24] P. Goddard, Nuovo Cim. A **4** (1971) 349.

[25] A. Erdélyi, W. Magnus, F. Oberhettunger, F. G. Tricomi, *Higher Transcendental Functions*, Bateman Manuscript Project, Volume 2, Chapter XIII, McGraw-Hill (1953).

[26] Z. Kunszt, A. Signer and Z. Trocsanyi, Nucl. Phys. B **411** (1994) 397 [arXiv:hep-ph/9305239]; For earlier calculations, see R. K. Ellis and J. C. Sexton, Nucl. Phys. B **269**, 445 (1986); Z. Bern and D. A. Kosower, Nucl. Phys. B **379**, 451 (1992).

[27] C. B. Thorn, Phys. Rev. **D82** (2010) 125021. [arXiv:1010.5998 [hep-th]].